

Research Article

Characterization of uridine-cytidine kinase like-1 nucleoside kinase activity and its role in tumor growth

Emily C. Matchett¹, Elise C. Ambrose¹ and  Jacki Kornbluth^{1,2}

¹Department of Pathology, Saint Louis University School of Medicine, St. Louis, MO, U.S.A.; ²VA St. Louis Health Care System, St. Louis, MO, U.S.A.

Correspondence: Jacki Kornbluth (jacki.kornbluth@health.slu.edu)



Uridine-cytidine kinase like-1 (UCKL-1) is a largely uncharacterized protein with high sequence similarity to other uridine-cytidine kinases (UCKs). UCKs play an important role in the pyrimidine salvage pathway, catalyzing the phosphorylation of uridine and cytidine to UMP and CMP, respectively. Only two human UCKs have been identified, UCK1 and UCK2. Previous studies have shown both enzymes phosphorylate uridine and cytidine using ATP as the phosphate donor. No studies have evaluated the kinase potential of UCKL-1. We cloned and purified UCKL-1 and found that it successfully phosphorylated uridine and cytidine using ATP as the phosphate donor. The catalytic efficiency (calculated as k_{cat}/K_M) was $1.2 \times 10^4 \text{ s}^{-1}, \text{ M}^{-1}$ for uridine and $0.7 \times 10^4 \text{ s}^{-1}, \text{ M}^{-1}$ for cytidine. Our lab has previously shown that UCKL-1 is up-regulated in tumor cells, providing protection against natural killer (NK) cell killing activity. We utilized small interfering RNA (siRNA) to down-regulate UCKL-1 *in vitro* and *in vivo* to determine the effect of UCKL-1 on tumor growth and metastasis. The down-regulation of UCKL-1 in YAC-1 lymphoma cells *in vitro* resulted in decreased cell counts and increased apoptotic activity. Down-regulation of UCKL-1 in K562 leukemia cells *in vivo* led to decreased primary tumor growth and less tumor cell dissemination and metastasis. These results identify UCKL-1 as a bona fide pyrimidine kinase with the therapeutic potential to be a target for tumor growth inhibition and for diminishing or preventing metastasis.

Introduction

Uridine-cytidine kinase (UCK) is a pyrimidine ribonucleoside kinase that catalyzes the phosphorylation of uridine and cytidine to their monophosphate forms, UMP and CMP, respectively [1–2]. This is the first step in the pyrimidine salvage pathway and is thought to be rate-limiting [3–4]. UMP and CMP are further phosphorylated by UMP-CMP kinase and nucleoside diphosphate kinases to UTP and CTP [3–5]. So far, only two human UCKs have been identified, UCK1 and UCK2 [6–8]. UCK1 is a 277 amino-acid protein with predicted molecular mass of 31 kDa and is universally expressed in healthy tissues. UCK2 is a 261 amino-acid protein with predicted molecular mass of 29 kDa and is restricted to human placenta and various tumor cells [3]. Human UCK1 and UCK2 show 72% sequence homology [3].

Uridine-cytidine kinase like-1 (UCKL-1) was first identified through its binding to Epstein-Barr virus encoded nuclear protein, EBNA-3 [9]. UCKL-1 is a 548 amino-acid protein [10]. The N-terminal half of UCKL-1 has high sequence similarity to both UCK1 and UCK2 and contains an ATP/GTP binding site like those found in the other UCKs [9]. The C-terminal half of UCKL-1 has sequence similarity to uracil phosphoribosyltransferase (UPRT) [9].

Studies conducted by our lab to identify proteins that regulate the anti-tumor activity of natural killer (NK) cells led to the identification of UCKL-1. NK cells play an important role in immune defense, recognizing and targeting tumor cells [11]. When NK cells encounter a target cell, cytolytic

Received: 12 November 2021
Revised: 26 April 2022
Accepted: 18 May 2022

Accepted Manuscript online:
18 May 2022
Version of Record published:
8 June 2022

granules, containing perforin and granzymes, are released and enter the target cell, leading to apoptosis [11]. We identified a novel protein found in the cytolytic granule membranes of NK cells called natural killer lytic-associated molecule (NKLAM). NKLAM is an E3 ubiquitin ligase, a member of the RING1-in between RING (IBR)-RING2 (RBR) protein family [11]. E3 ubiquitin ligases regulate the ubiquitination of proteins by catalyzing the transfer of activated ubiquitin from an E2 ubiquitin conjugating enzyme to its substrate [11]. Ubiquitination is an important post-translational modification, targeting proteins for degradation by proteasomes or altering their cellular localization and function [12–14].

Using the yeast two-hybrid system, we identified UCKL-1 as a substrate for NKLAM [10]. Overexpression studies in HEK293 cells showed coprecipitation of NKLAM and UCKL-1 and interaction between the two led to decreased expression of UCKL-1 [10]. Colocalization studies confirmed that UCKL-1, in the presence of NKLAM, translocates from the nucleus to the cytoplasm, where it is ubiquitinated and degraded [10]. Due to its homology to other UCKs, we investigated the involvement of UCKL-1 in proliferation and survival of tumor cells. Down-regulation of UCKL-1 in K562, a human erythroleukemia cell line, resulted in decreased tumor cell proliferation and increased spontaneous apoptosis and susceptibility to NK cell lysis [15]. Overexpression of UCKL-1 *in vitro* provided protection of K562 cells from NK cell lysis [16]. *In vitro* and *in vivo* overexpression of UCKL-1 in RMA-S cells, a mouse lymphoma cell line, also increased their resistance to NK cell lysis [16].

Several studies have identified UCKL-1 as a potential biomarker, with increased expression in prostate cancer [17], breast cancer [18], colorectal cancer [19], hepatocellular carcinoma [20], and lung cancer [21]. Additionally, overexpression of UCK2 was reported in various tumor cells. One study demonstrated that UCK2 overexpression in breast cancer tissue correlated with a less differentiated phenotype and shorter survival time among patients with breast cancer [22]. Another study found that patients with high UCK2 expression in hepatocellular carcinoma tissues had more aggressive clinicopathological features and poorer prognosis compared with those with low UCK2 expression [23]. There have been no studies to date identifying UCK1 as a prognostic marker in cancer.

Other investigators characterized the kinase activity of UCK1 and UCK2. Van Rompay et al. [3] reported that the K_M values for UCK2 were 4- to 6-fold lower for uridine and cytidine, respectively, compared with the K_M values for UCK1. The V_{max} values for UCK2 were several-fold higher than UCK1 [3]. Catalytic efficiency, calculated as k_{cat}/K_M , showed both uridine and cytidine were more efficient substrates for UCK2 than UCK1 [3]. Meinsma and Van Kuilenburg also compared UCK1 and UCK2 kinase activity. Although both proteins were expressed in a panel of neuroblastoma cell lines, the V_{max} of UCK2 was 22- and 8-fold higher with uridine and cytidine, respectively, compared with UCK1 [8]. The K_M of UCK1 was 39- and 40-fold higher with uridine and cytidine, respectively, compared with UCK2 [8]. Catalytic efficiency showed uridine and cytidine were more efficient substrates of UCK2 than UCK1 [8]. To date, no studies have characterized the kinase properties of UCKL-1.

The present investigation was initiated to determine whether UCKL-1 has pyrimidine kinase activity and to further investigate its role in tumor cell growth both *in vitro* and *in vivo*. We focused our comparison of UCKL-1 kinase activity with UCK2 due to UCK2's efficient catalytic activity, its selective expression in tumor cells, and the identification of both UCKL-1 and UCK2 as potential biomarkers in multiple cancer types. We cloned human UCKL-1 with two polyhistidine tags and purified the recombinant protein by immobilized metal affinity chromatography (IMAC). Phosphorylation of uridine and cytidine was analyzed using an enzymatic assay. We demonstrated that UCKL-1 catalyzes the phosphoryl transfer from ATP to uridine and cytidine similarly to UCK2. We determined the involvement of UCKL-1 in murine cancer cell apoptosis and proliferation *in vitro* utilizing YAC-1 mouse lymphoma cells. We investigated the effects of down-regulation of UCKL-1 on primary tumor growth and metastasis *in vivo* using green fluorescent protein (GFP)-expressing K562 leukemia tumor cells in immunodeficient mice. UCKL-1 down-regulation in tumor cells reduces tumor growth and increases apoptosis *in vitro* and *in vivo* and decreases tumor dissemination and metastasis *in vivo*.

Results

Comparison of UCKL-1 with UCK1 and UCK2

To date, two human UCKs have been cloned, purified, and tested for enzymatic activity. Due to its homology to UCK1 and UCK2, UCKL-1 was presumed to have similar activity, but its kinase function had not been evaluated. Figure 1 shows the alignment of UCKL-1 with UCK1 and UCK2 protein sequences. Regions of

UCKL1	MAAPPARADADPSPTSPPTARDTPGRQAEKSETACEDRSNAESLDRLLPFVGTGRSPRKR	60
	ATP binding	
UCKL1	TTSQCKSEPPLLRRTSKRTIYTAGRPPWYNEHGTQSKEAFAIGLGGSSASGKTIIVARMIIE	120
UCK1	-----MASAGGEDCESPAPEADRPHQRPFLLIGVSGGTASGKSTVCEKIME	45
UCK2	-----MAGDSEQTLQNHQQPNGGEPFLIGVSGGTASGKSSVCAKIVQ	42
UCKL1	ALDV-----PWVLLSMDSFYKVLTEQQQEQAAHNNFNFDHPDAFDFDLIIISTLKKLK	173
UCK1	LLGQNEVEQRQRKVVILSQDRFYKVLTAEQKAKALKGQYNFDHPDAFDNDLMHRTLKNIV	105
UCK2	LLGQNEVDYRQKQVVILSQDSFYRVLTSEQKAKALKGQFNFDHPDAFDNELILKTLKEIT	102
UCKL1	QGKSVKVPITYDFTHSRKKDWKTLYGANVIFEGIMAFADKTLELLDMKIFVDTDSDIR	233
UCK1	EGKIVEVPTYDFVTHSRLPETTVVYPADVVLFEGLLVFYSQEIIRDMFHLRLEFVDTDSVDR	165
UCK2	EGKTVQIPVYDFVSHSRKEETVTVYPADVVLFEGLLAFYSQEVRLDFQMKLEFVDTDADTR	162
UCKL1	LVRRLRRDISERGRDIEGVIKQYNKFKVPSFDQYIQPTMRIADIVVPRGSGNTVAIDLIV	293
UCK1	LSRRVLRDV-RRGRDLEQILTQYTTFFVKPAFEEFCLPTKKYADVII PRGVDMVAINLIV	224
UCK2	LSRRVLRDISERGRDLEQILSQYITFFVKPAFEEFCLPTKKYADVII PRGADNLVAINLIV	222
UCKL1	QHVSQLEERELSVRAALASAHQCHPLPRTL SVLKSTPQVRGMHTIIR---DKETS RDEF	350
UCK1	QHIQDILNGDICKWHRGGSNG---RSYKRTFSEPGD---HPGMLTSGKRSHLESSSRPH-	277
UCK2	QHIQDILNGGPKSRQQTNGCL-----NGYTPSRKRQASESSSRPH-	261
UCKL1	IFYSKRLMRLLEHALSFLPFQDCVVQTPQGQDYAGKCYAGKQITGVSILRAGETMEPAL	410
UCKL1	RAVCKDVRI GTILIQTNQLTGEPELHYLRPKDISDDHVILMDCTVSTGAAAMMAVRVLL	470
UCKL1	DHDVPEDKIFLLSLLMAEMGVHSVAYAFPRVRIITTAVDKRVNDLFRIPGIGNFGDRYE	530
UCKL1	GTDAVPDGSDEEEVAYTG	548

Figure 1. Alignment of human UCKL-1, UCK1, and UCK2.

Human UCKL-1 (UniprotKB Q9NWZ5), UCK1 (Q9HA47) and UCK2 (Q9BZX2) were aligned using the Clustal program. Identical amino acids among the three proteins are highlighted in yellow. Similar amino acids between UCKL1 and either UCK1 or UCK2 are depicted in red. The boxed amino acids represent the ATP binding site. The section of UCKL-1 highlighted in blue has 41% similarity to human UPRT (Q96BW1).

homology are depicted in yellow while amino acid similarities are shown in red. Between amino acids 78 and 296 of UCKL-1, there is 44% identity among all 3 proteins. There is 76% amino acid similarity between UCKL-1 and either UCK1 or UCK2, including the ATP/GTP binding site. Amino acids 329–533 of UCKL-1 have 41% similarity with human UPRT (sequence highlighted in blue). UCKL-1 and UCK2 are both expressed in tumor cells, and high levels have been associated with poor prognosis for patients with a variety of cancers. We therefore sought to compare the kinase activity of UCKL-1 and UCK2.

Purification of UCKL-1 and UCK2

Plasmids expressing UCKL-1 and UCK2 with two polyhistidine tags were transformed into *E. coli* BL21-DE3 competent cells and the recombinant proteins were purified by IMAC. An amount of 100 ng of each purified protein was run on a 10% SDS-polyacrylamide gel and transferred to a PVDF membrane. The membrane was probed with anti-UCKL-1 and UCK2 antibodies. An additional gel was stained with Coomassie blue. The expected molecular weight of His-tagged UCKL-1 is 80 kDa, and His-tagged UCK2, 48 kDa.

Figure 2A shows Coomassie blue staining of a representative gel. Single bands corresponding to UCKL-1 and UCK2 confirmed the success of isolation and purification of the recombinant proteins. Additionally, immunoblot analysis confirmed the isolation and purity of UCKL-1 and UCK2 (Figure 2B–D). Antibody against UCKL-1 has no cross-reactivity with UCK2 (Figure 2C), and the antibody against UCK2 has no cross-reactivity against UCKL-1 (Figure 2D).

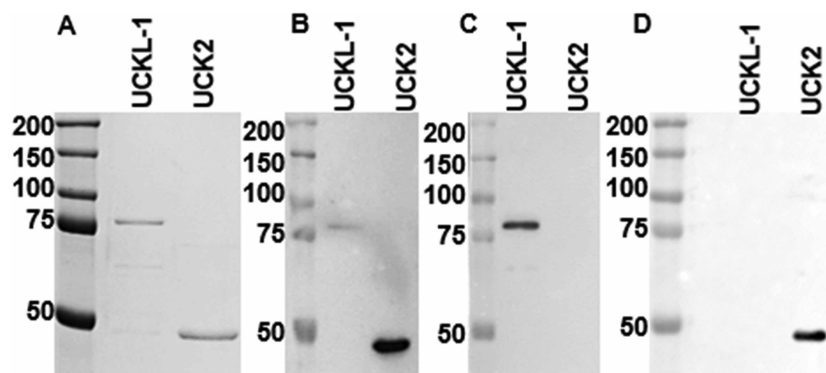


Figure 2. Purification of bacterially expressed His-tagged UCKL-1 and UCK2.

(A) Coomassie blue stained gel of 100 ng of purified UCKL-1 (lane 1) and UCK2 (lane 2). Single band detected for each: UCKL-1 at 80 kDa and UCK2 at 48 kDa. (B) Western blot analysis with His antibody confirmed purity and isolation of His-tagged UCKL-1 (lane 1) and UCK2 (lane 2). (C) Analysis with UCKL-1 (B-11) antibody (lane 1) showed no cross-reactivity with UCK2 (lane 2). (D) Analysis with UCK2 antibody (lane 2) showed no cross-reactivity with UCKL-1 (lane 1). Blots represent 1 of 3 experiments with identical results.

Enzymatic activity of UCKL-1

We conducted an enzymatic assay to determine whether UCKL-1 has pyrimidine kinase activity, and if so, to compare the activity of UCKL-1 to UCK2. We utilized the ADP-Glo™ Kinase Assay system, in which the luminescent signal generated is directly proportional to the ADP produced during the kinase reaction and correlates with kinase activity [24].

Initially, we optimized the assay system for UCK2. We detected UCK2 pyrimidine kinase activity consistent with that reported by others [3,8]. Using conditions that were maximal for UCK2 activity, we were unable to detect UCKL-1 kinase activity. When changes in pH, salt concentration, and temperature were made, we were able to successfully measure UCKL-1 kinase activity. Both enzymes efficiently phosphorylated uridine and cytidine (Figure 3). UCKL-1 exhibited a K_M value of $3.4 \times 10^{-2} \mu\text{M}$ for uridine and $6.5 \times 10^{-2} \mu\text{M}$ for cytidine. These values were several-fold higher for UCK2 (Table 1). UCK2 exhibited V_{max} values several-fold higher than those for UCKL-1. The catalytic efficiency, calculated as k_{cat}/K_M , for UCK2 was 5-fold higher with cytidine compared with UCKL-1. There was no difference between the catalytic efficiency of UCK2 and UCKL-1 with uridine as the substrate.

Expression of UCKL-1, UCK1, and UCK2 in tumor cells

UCK1 and UCK2 are expressed in various tumor cell lines, including K562 cells [8,18,25]. We sought to evaluate the expression of UCKL-1, UCK1, and UCK2 in a panel of tumor cell lines. Lysates from seven human tumor cell lines (U-87 glioblastoma, K562 erythroleukemia, Jurkat T cell leukemia, Huh-7 hepatocellular carcinoma, U-2 OS bone osteosarcoma, MDA-MB-231 triple negative breast adenocarcinoma, and MCF-7 breast adenocarcinoma) and one mouse tumor cell line (YAC-1 lymphoma) were prepared and subjected to immunoblot analysis. The molecular weight of endogenous UCKL-1 is 61 kDa, endogenous UCK1 is 31 kDa, and endogenous UCK2 is 29 kDa. Actin was used as loading control. Immunoblot analysis (Figure 4) showed the presence of all three UCKs in this panel of tumor cell lines, with varying levels of expression.

Decreased growth of siUCKL-1 treated cells

Previously, we found that down-regulation of UCKL-1 in K562 cells by RNA interference resulted in increased apoptosis and decreased proliferation [15]. To determine if this function of UCKL-1 was similar across human and mouse cell lines, we nucleofected YAC-1 cells with either UCKL-1 siRNA (siUCKL-1) or control siGFP (siGFP). There were significantly fewer YAC-1 cells treated with siUCKL-1 compared with siGFP-treated cells after 24 h of culture (Figure 5A). These results correspond with those seen previously with K562 [15].

To determine if the lower cell numbers seen in siUCKL-1-treated cultures compared with siGFP-treated cultures were due to cell death via apoptosis, we measured caspase 3/7 activity in each group. YAC-1 cells with down-regulated UCKL-1 had significantly more caspase activity than siGFP-treated cells (Figure 5B). This

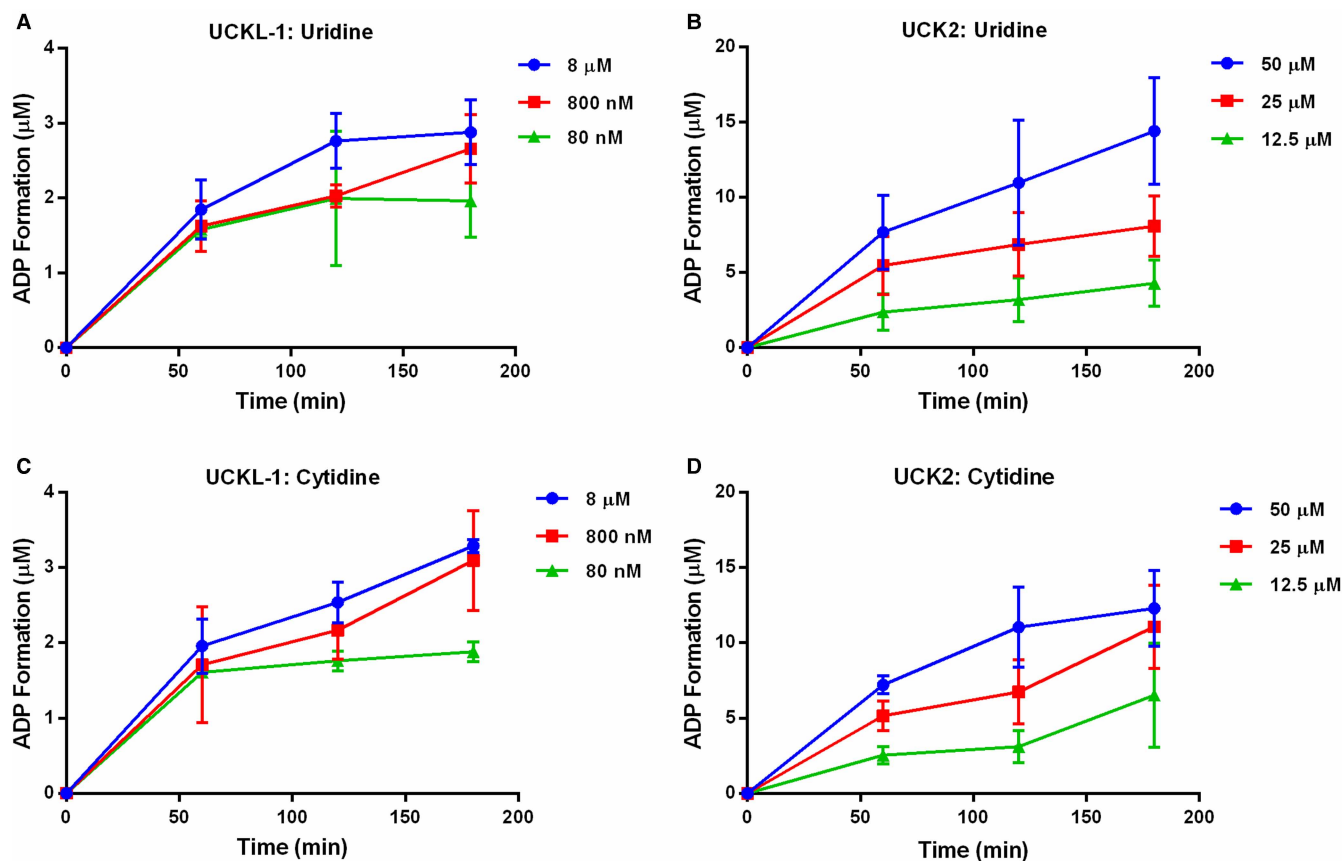


Figure 3. Pyrimidine kinase activity of UCKL-1 and UCK2.

Purified UCKL-1 (500 ng) and UCK2 (1 ng) were dispensed into 384-well plates and mixed with a substrate/ATP buffer. Final concentration of ATP was 100 μM . ADP formation was measured at various substrate concentrations. (A) UCKL-1 with uridine as substrate; (B) UCK2 with uridine as substrate; (C) UCKL-1 with cytidine as substrate; (D) UCK2 with cytidine as substrate. Kinase reactions were measured at 0, 60, 120, and 180 min. Luminescence at each time point was converted to the amount of ADP formed during the kinase reaction using an ATP-to-ADP conversion curve. ADP formation was plotted versus time. Each data point represents the mean \pm SD of 3–5 replicates.

corresponds with results seen in caspase activity of K562 cells with down-regulated UCKL-1 [15]. Therefore, the effect of UCKL-1 down-regulation appears to be similar across mouse and human tumor cells, with higher levels of apoptotic activity observed in both K562 cells and YAC-1 cells treated with siUCKL-1 [15].

Effect of UCKL-1 down-regulation on primary tumor growth and metastasis *in vivo*

To evaluate the effect of UCKL-1 down-regulation on primary tumor growth and metastasis, we injected K562-GFP cells subcutaneously in the rear flank of immunodeficient NOD-scid IL2R γ^{null} (NSG) mice. For

Table 1 Enzymatic properties of the recombinant proteins, UCKL-1 and UCK2, with ATP as phosphate donor

Substrate	K_M (μM)		V_{max} ($\mu\text{mol}/\text{mg}/\text{min}$)		k_{cat}/K_M ($\text{s}^{-1}, \text{M}^{-1}$)	
	UCKL-1	UCK2	UCKL-1	UCK2	UCKL-1	UCK2
Uridine	3.4×10^{-2}	207.3	3.1×10^{-4}	3.98	1.2×10^4	1.5×10^4
Cytidine	6.5×10^{-2}	25.07	3.5×10^{-4}	1.09	0.7×10^4	3.5×10^4

k_{cat} was calculated using molecular mass of 80 kDa for UCKL-1 and 48 kDa for UCK2.

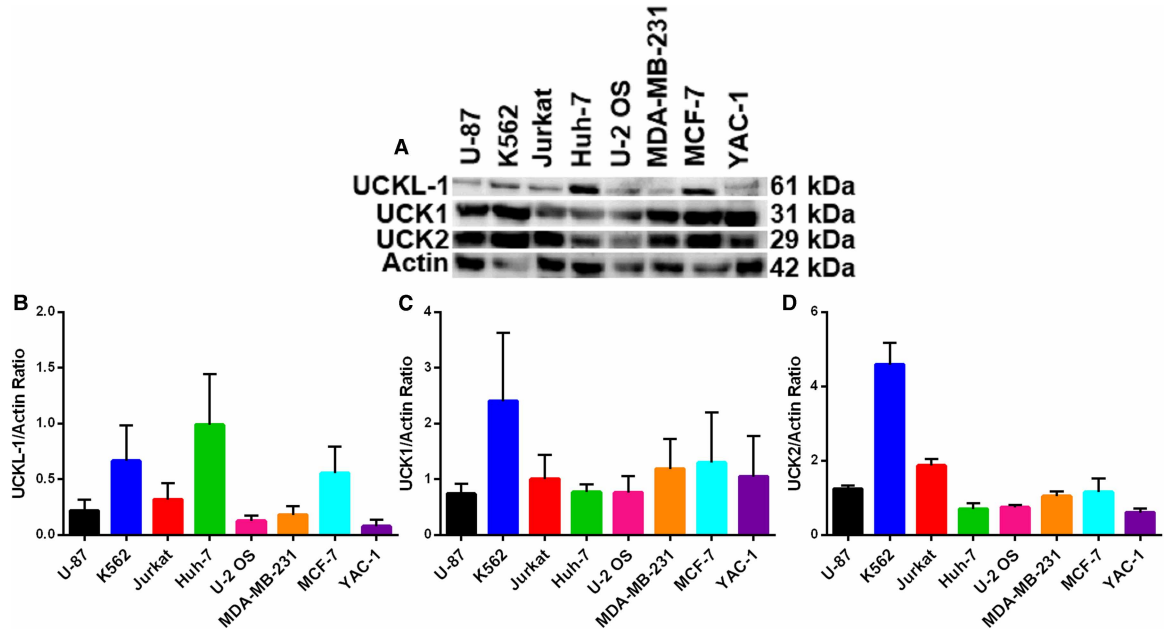


Figure 4. Immunoblot analysis of UCKL-1, UCK1, and UCK2 expression in various tumor cell lines.

(A) Whole-cell lysates were prepared and UCKL-1, UCK1, and UCK2 were detected by immunoblotting. Actin was used as a loading control. (B–D) Densitometric analysis of UCKL-1, UCK1, and UCK2 expression relative to actin for each cell line (mean \pm SD, $n = 3$).

primary tumor growth studies, mice were injected with tumor cells into both flanks. This reduced tumor size variability among the mice. Once tumors were established (day 8), scrambled siRNA (sicontrol) or siUCKL-1 was injected intratumorally every other day. Tumors on one flank were treated with sicontrol and the other side with siUCKL-1. siUCKL-1-injected primary tumors were significantly smaller than sicontrol-injected tumors at day 10, 12, 14, and 15 (Figure 6A). After 15 days, mice were sacrificed, photographed (Figure 6C) and tumors excised and weighed. All animals survived until end of study and none were withdrawn prior to its completion. siUCKL-1-injected primary tumors weighed 2.5-fold less than sicontrol-injected tumors (Figure 6B).

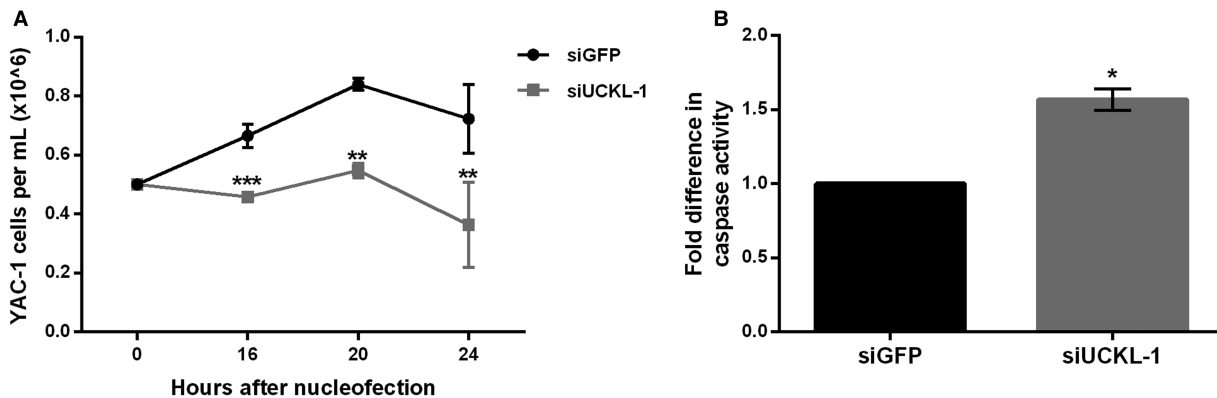


Figure 5. Down-regulation of UCKL-1 in YAC-1 cells induces apoptosis.

(A) YAC-1 cells were nucleofected with either siGFP control (siGFP) or siUCKL-1. Cell counts were significantly lower at 16, 20, and 24 h after nucleofection of siUCKL-1 compared with siGFP (mean \pm SD, $n = 5$, * $P \leq 0.02$, ** $P \leq 0.002$, *** $P \leq 0.0002$). UCKL-1 down-regulation was confirmed by real-time PCR 24 h after nucleofection. (B) YAC-1 cells nucleofected with siUCKL-1 had more caspase 3/7 activity than siGFP-treated cells (mean \pm SD, $n = 4$, * $P \leq 0.02$). Caspase activity was determined by a luminescent assay and UCKL-1 down-regulation confirmed by real-time PCR.

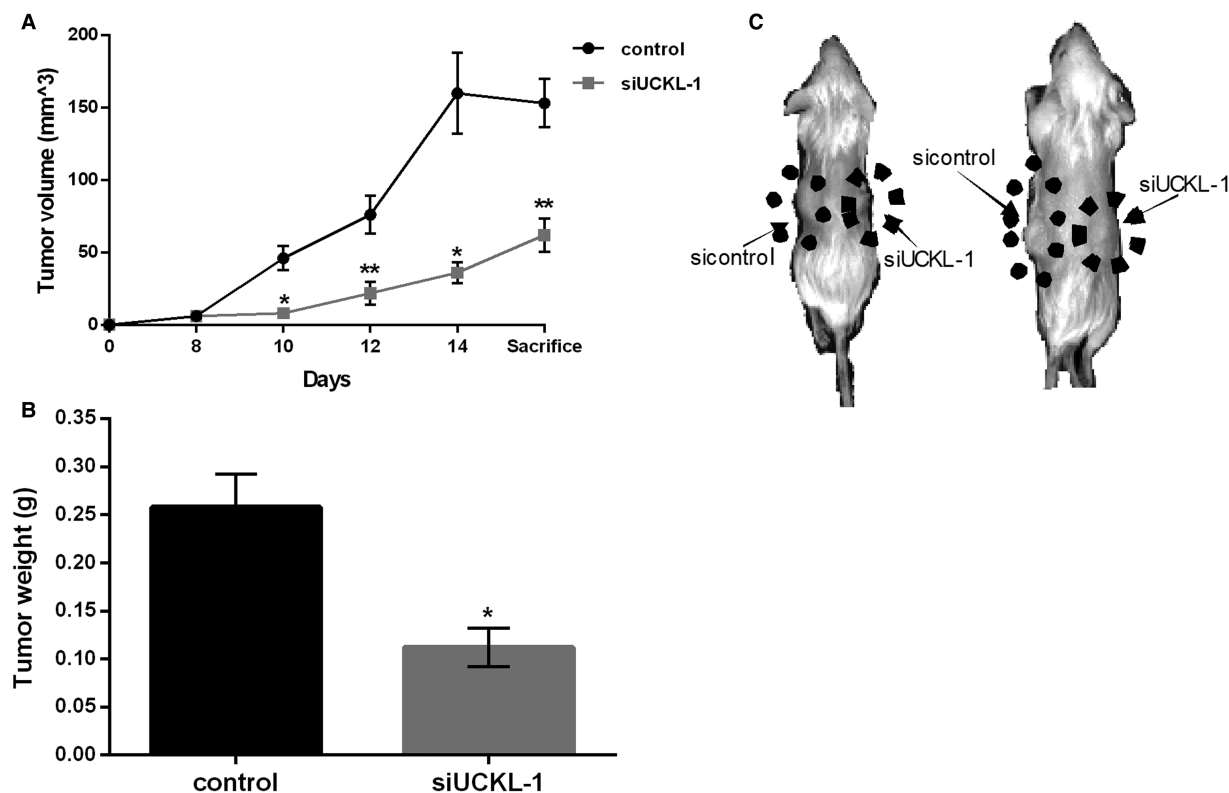


Figure 6. UCKL-1 down-regulation inhibits primary tumor growth in NSG mice.

(A) 10^6 K562-GFP cells suspended in Matrigel were injected into the right and left flanks of NSG mice. Once tumors were established (day 8), either 8 μ g scrambled siRNA (sicontrol) or UCKL-1 siRNA (siUCKL-1) in 50 μ l PBS was injected intratumorally. Tumors were measured and injected with siRNA every other day for one week. Significantly less tumor growth was seen in the siUCKL-1-injected tumors at day 10, 12, 14, and day of sacrifice (day 15) (mean \pm SD, $n = 18$, * $P \leq 0.001$, ** $P \leq 0.0005$). (B) Subcutaneous tumors were extracted from NSG mice on day 15 and weighed. SiUCKL-1-injected tumors weighed significantly less than sicontrol-injected tumors (mean \pm SD, $n = 18$, * $P \leq 0.001$). (C) Representative images of NSG mice at sacrifice. The siUCKL-1-injected subcutaneous tumor on the right flanks of the mice were visibly smaller than the sicontrol-injected tumor on the left. Two representative mice are shown.

The expression of GFP by K562 cells allowed for tumor visualization within the mouse. Figure 7 shows expression of GFP by the subcutaneous tumors in the rear flank of a representative mouse. The siUCKL-1-injected tumor was visibly smaller than the sicontrol-injected tumor *in vivo* (Figure 7, left) and after extraction from the mouse (Figure 7, right). The GFP expression level in siUCKL-1-injected tumors was 3-fold lower than in sicontrol-injected tumors.

Since we observed a difference in primary tumor growth, we examined the effect of UCKL-1 down-regulation on the level of lung metastasis and tumor dissemination. For these studies, mice were injected subcutaneously on one side with K562-GFP cells. Each mouse was injected intratumorally with either sicontrol or siUCKL-1. Lung metastasis was determined by the level of GFP expression in the lungs using qPCR, which reflects the number of K562-GFP cells present. Mice in which the primary tumor was injected with siUCKL-1 had 5-fold less lung GFP expression than sicontrol-injected mice (Figure 8A). Less GFP expression was also observed in the blood of siUCKL-1-injected mice (Figure 8B). No GFP was detected in the lungs or blood of non-tumor bearing mice. Therefore, decreasing UCKL-1 expression in primary tumors through siRNA delivery impacted primary tumor growth, lung metastasis, and release of tumor cells into circulation.

Primary tumors were harvested, fixed, paraffin embedded, sectioned, and analyzed for levels of terminal deoxynucleotidyl transferase dUTP nick end labeling (TUNEL) to quantitate DNA damage, reflective of apoptosis. *In vitro* siUCKL-1 treatment of K562 induced apoptosis [15]. A similar effect on apoptosis was observed *in vivo*. Tumors injected with siUCKL-1 had greater TUNEL staining (measured as positive pixel area) than

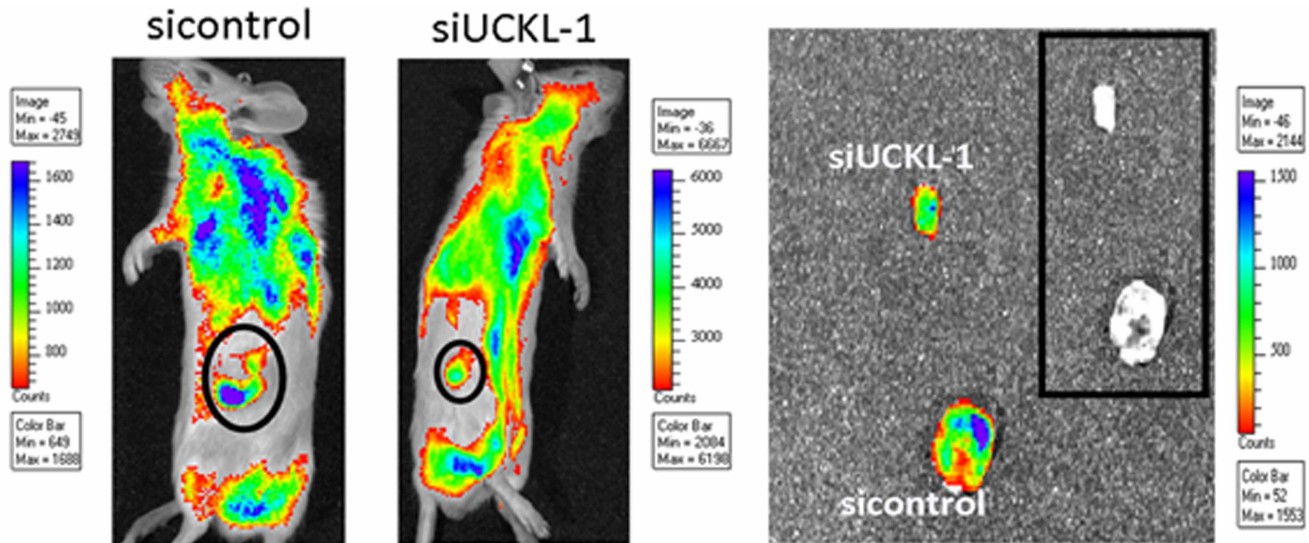


Figure 7. Diminished growth of siUCKL-1 treated tumors *in vivo*.

NSG mice were injected subcutaneously with K562-GFP tumor cells on both rear flanks. Tumors were injected with either scrambled (sicontrol) or UCKL-1 siRNA (siUCKL-1) every other day and measured. Representative IVIS images of NSG mice showed less growth of siUCKL-1-injected tumors. Tumors were visible by GFP both in the mouse (left) and after extraction (right). The levels of GFP were analyzed by IVIS software and quantitated by photon efficiency. There was 3-fold less GFP expression in the siUCKL-1 tumors compared with the sicontrol tumors ($n = 18$).

those injected with control siRNA. siUCKL-1-injected tumors had 10-fold more apoptosis than sicontrol-injected tumors (Figure 9). These results indicate that decreasing UCKL-1 expression in tumor cells induces apoptosis and inhibits tumor growth, dissemination, and metastasis.

Discussion

We previously identified UCKL-1 as a substrate for ubiquitination by NKLAM, an E3 ligase important in NK cell anti-tumor activity [10]. UCKL-1 was first identified by Kashuba et al. [9] through its binding to Epstein-

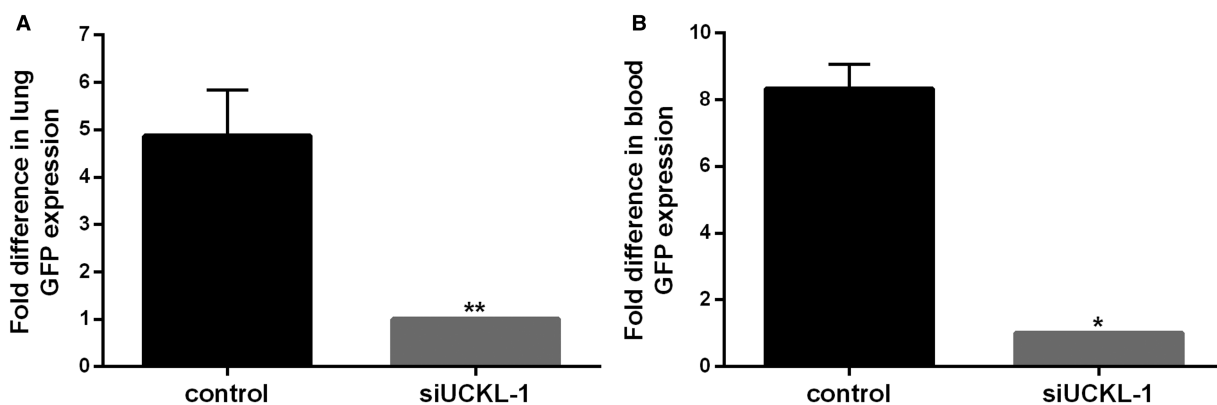


Figure 8. Less lung metastasis and fewer circulating tumor cells in mice receiving intratumoral injections of siUCKL-1.

(A) Lungs from tumor-bearing NSG mice were extracted and analyzed for GFP expression by quantitative RT-PCR. GFP expression correlates with the number of K562-GFP tumor cells present. The level of lung metastasis was significantly lower in mice injected with siUCKL-1 than in sicontrol-injected mice (mean \pm SD, $n = 34$, $** P \leq 0.01$). (B) At time of sacrifice, 500 μ l blood was removed from the heart. RNA was extracted and analyzed for GFP by quantitative RT-PCR. Mice bearing siUCKL-1-injected tumors had significantly fewer circulating tumor cells than mice bearing sicontrol-injected tumors (mean \pm SD, $n = 13$, $* P \leq 0.04$). No GFP expression was detected in mice without tumor present.

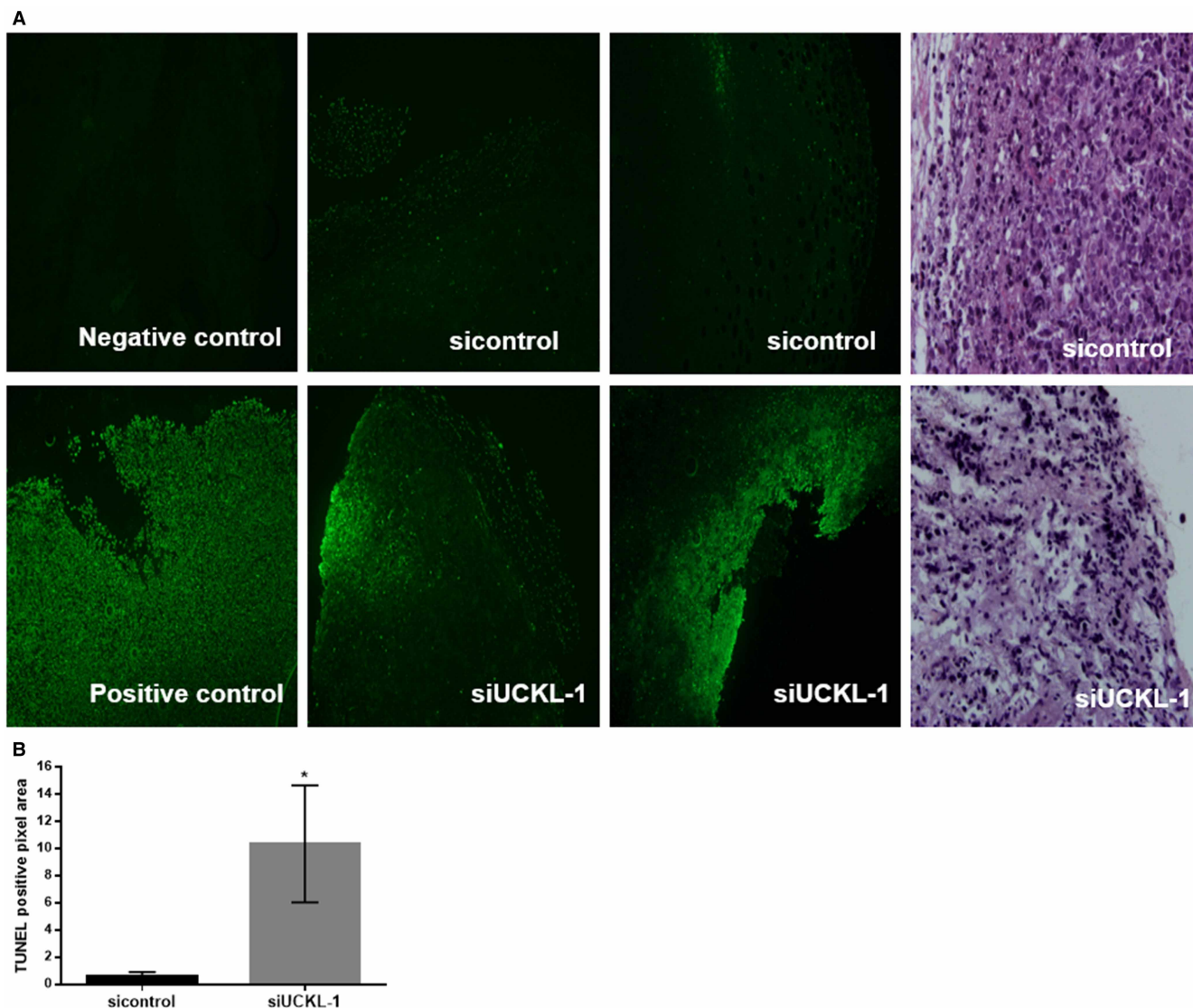


Figure 9. Higher levels of apoptosis in UCKL-1 down-regulated K562 tumors *in vivo*.

(A) Tumors isolated from NSG mice were fixed, paraffin embedded, sectioned, and subjected to fluorescent TUNEL staining, which visualizes nicks in the DNA and is reflective of apoptosis. A negative control and positive control (DNase treatment) were used for background and positive staining determination, respectively. TUNEL staining is depicted in green. Representative images are shown. siUCKL-1-injected tumors had higher levels of apoptosis than sicontrol-injected tumors. The two right panels are Hematoxylin and Eosin staining of the tumors. (B) Quantitative analyses of TUNEL staining. The TUNEL positive pixel area of six fields was analyzed for each tumor sample and normalized to negative control background staining. siUCKL-1-injected tumors had significantly more TUNEL fluorescent staining (mean \pm SD, $n = 8$, * $P \leq 0.05$).

Barr virus nuclear antigen 3 protein (EBNA-3). They theorized UCKL-1 was a novel uridine kinase (UK)/uracil phosphoribosyltransferase (UPRT; UK/UPRT), an enzyme with dual catalytic activity. UCKs are pyrimidine ribonucleoside kinases that catalyze the phosphorylation of uridine and cytidine to their monophosphate forms, while UPRT catalyzes the conversion of uracil to UMP [1,26]. Both enzymes play an integral role in the pyrimidine salvage pathway [1,26]. The N-terminal half shows high sequence similarity to other UCKs containing an ATP/GTP binding site (Figure 1) [9]. The crystal structure of UCKL-1 suggests high homology to UPRT in its C-terminal end. It was reported that UCKL-1 mRNA is ubiquitously expressed throughout the body, including the brain, placenta, lung, liver, and pancreas, with higher levels found in skeletal muscle, heart, and kidney [9]. Even higher levels of UCKL-1 are found in tumor cells, especially those with the most

aggressive phenotype [17–21]. To date, there have been no studies performed to characterize UCKL-1 kinase function.

We expressed human UCKL-1 and UCK2 in bacteria to characterize and compare the pyrimidine kinase activity of the two enzymes. We analyzed the phosphorylation of both uridine and cytidine with ATP as the phosphate donor. The catalytic efficiency of UCK2 with cytidine was 5-fold higher than that observed for UCKL-1. There was no difference in the catalytic efficiency of UCK2 and UCKL-1 with uridine (Table 1). The observed K_M and V_{max} values for UCK2 were comparable to those reported previously [3,8,25]. Both uridine and cytidine were determined to be more efficient substrates for UCK2 than UCK1 [3,8]. Based upon the previously published data comparing the kinase activity of UCK1 and UCK2, our results suggest that UCKL-1 is a more efficient enzyme than UCK1. Further experiments are in progress to compare all three UCKs. We are also examining whether UCKL-1 has UPRT activity.

UPRTs have mostly been characterized in lower organisms, including *Mycobacterium tuberculosis* and *Toxoplasma gondii*, as well as in the plant species, *Arabidopsis thaliana*. [26–28]. *Arabidopsis thaliana* expresses a dual-domain UK/UPRT (AtUK/UPRT) [28]. The N-terminal region contains a UK domain with an ATP binding motif, and the C-terminal domain consists of a UPRT domain. Sequence analysis revealed 50% homology to human UCKL-1 for both domains [28]. AtUK/UPRT was transformed into *E. coli* and mutated in *Arabidopsis*. In both cases, the protein was functional, displaying both UK and UPRT activity. These findings indicate that UPRT and UK play a role in nucleotide metabolism in plants through the pyrimidine salvage pathway [28].

There has been minimal research characterizing human UPRT. One study attempted to characterize human UPRT isolated from fetal brain [29]. After purification, the yielded protein was catalytically inactive *in vitro*. The authors suggested that other unknown factors might be necessary for human UPRT to function properly *in vivo* [29]. They reported, during their first attempts at purifying human UPRT, the protein formed inclusion bodies after IPTG induction at 37°C [29].

Recombinant UCKL-1 initially also formed inclusion bodies after IPTG induction at 37°C. We had to optimize conditions to increase protein yield. Additionally, we had to optimize conditions for the enzymatic assays. Previous studies of UCK2 used a reaction buffer containing 50 mM Tris, pH 7.5, 5 mM MgCl₂, 2 mM DTT, and 0.5 mg/ml BSA [25]. We utilized this reaction buffer for our UCK2 enzymatic reactions, and the results correlated with those of a similar study [25]. However, we had to adjust the pH, salt concentration, and temperature of the reaction to measure the kinase activity of UCKL-1. This indicates that these enzymes have distinctly different requirements for function.

Reports have shown endogenous expression of UCK1 and UCK2 in human tumor tissues, but there has been no investigation into the endogenous expression of UCKL-1 across different tumor cell lines [8,22,23]. We show UCKL-1 is expressed in multiple types of cancer cells (Figure 4). These results encourage further investigation into UCKL-1 as a prognostic biomarker of cancer.

Our lab explored the effect of down-regulating UCKL-1 in K562 cells *in vitro*. This resulted in decreased tumor cell proliferation and increased susceptibility to NK cell lysis [15]. We then questioned whether similar effects of down-regulating UCKL-1 would occur in other tumor cell lines. We nucleofected YAC-1 cells, a mouse lymphoma cell line, with either control (siGFP) or UCKL-1 siRNA. There were significantly lower numbers of siUCKL-1-treated cells compared with siGFP-treated cells 24 h after nucleofection (Figure 5). Down-regulation of UCKL-1 resulted in increased caspase activity at 20 h after treatment (Figure 5). These results correspond with those observed previously in K562 cells [15], leading us to conclude that the effect of UCKL-1 down-regulation is similar across species and cell lines. There is variation in the degree of response to down-regulation of UCKL-1 among different cell lines, and this is most likely due to varying levels of UCKL-1 expression as well as variation in the expression of other UCKs.

We sought to examine the role of UCKL-1 *in vivo*. In this study, we used K562, a human erythroleukemia cell line, to determine the effect of UCKL-1 down-regulation. We injected either control or UCKL-1 siRNA directly into K562 tumors established in NSG mice every other day to enhance effectiveness of the siRNA and maintain UCKL-1 knockdown. Some of the studies in NSG mice were conducted with mice bearing double tumors; one tumor was injected with control siRNA, while the other was injected with UCKL-1 siRNA. In mice bearing double tumors, we observed a significant difference in primary tumor size between the siUCKL-1-treated tumors and the control-treated tumors (Figure 6). The UCKL-1 down-regulated tumors grew slower, were smaller, and weighed less than the sicontrol-treated tumors (Figure 6). Another study was performed with mice bearing single tumors; each tumor was injected with either control or UCKL-1 siRNA. We

also observed a decrease in primary tumor growth, as well as less lung metastasis and fewer circulating tumor cells (Figure 8).

Down-regulation of UCKL-1 in K562 cells *in vitro* enhanced their susceptibility to apoptosis [15]. Greater apoptotic activity in UCKL-1 down-regulated cells was also evidenced *in vivo* by TUNEL staining of siUCKL-1-treated tumors (Figure 9). To eliminate the possibility that the smaller tumor size was the reason for higher levels of apoptosis, similarly sized control and siUCKL-1-injected tumors underwent TUNEL staining. Despite the tumors being the same size, UCKL-1 down-regulated tumors had higher levels of apoptosis than control tumors. It is likely that the high level of apoptosis in cells with decreased UCKL-1 expression was, in part, responsible for the lower primary tumor growth rate and less lung metastasis and tumor dissemination. We plan to conduct further *in vitro* and *in vivo* experiments down-regulating and overexpressing UCKL-1 in other tumor models to assess tumor growth rates and dissemination. We also want to compare the functional activity of UCKL-1 with UCK2 in tumor cells. We plan to investigate whether the down-regulation of both UCKL-1 and UCK2 would have a greater effect on tumor growth and survival than either alone.

Studies have highlighted UCKL-1's potential as a biomarker in numerous cancer cell types [17–21]. Greater than 80% of cancers demonstrate significantly increased expression of pyrimidine metabolism-related genes compared with normal tissues [30]. This includes genes that regulate both the pyrimidine *de novo* and salvage pathways. More than two decades ago, inhibitors of *de novo* pyrimidine synthesis were developed for potential use in cancer therapy [31]. Pharmacological inhibition of dihydroorotate dehydrogenase (DHODH), which is the fourth of six universally conserved enzymatic reactions in the pyrimidine *de novo* synthetic pathway, was reported to reduce liver metastasis in colorectal cancer and small cell lung cancer models [32–34]. DHODH inhibitors significantly decreased levels of leukemia-initiating cells, and improved survival of leukemia-bearing mice [35]. It was soon discovered that cancer cells could escape the *de novo* synthesis pathway and adapt the nucleotide salvage pathway for DNA replication and cell proliferation [31]. Researchers turned their focus to the salvage pathway for targeted cancer treatment, but eventually this was set aside because of limitations translating *in vitro* studies into *in vivo* and clinical studies [31]. In the last few years, there has been a reemergence of interest in targeting the pyrimidine salvage pathway due to the development of new inhibitors [31]. Sarkisjan et al. found that the novel cytidine analog fluorocyclopentenylcytosine (RX-3117) is activated by UCK2 only. UCK1 does not play a role in this process [36]. Once activated, RX-3117 is incorporated into the DNA or RNA of cancer cells and induces apoptosis [37]. In our studies, down-regulation of UCKL-1 in K562 leukemia cells *in vivo* resulted in less tumor dissemination and metastasis. These findings suggest that inhibiting the pyrimidine salvage pathway in tumors may be another therapeutic strategy to treat cancer patients and encourage a fresh look into targeting the salvage pathway, including developing agents that inhibit UCKL-1.

Another emerging area of interest for pyrimidine biosynthesis is its potential as a target for antiviral therapy. Liu et al. reported a combination treatment of GSK983, a broad-spectrum antiviral agent, and cyclopentenyl uracil (CPU), an inhibitor of uridine salvage, suppressed dengue virus replication in the presence of physiological uridine concentrations. These findings are intensifying studies to develop specific inhibitors against UCKs [38]. In summary, our data demonstrate that UCKL-1 is a pyrimidine kinase. It is expressed in multiple tumor cell lines and plays a role in tumor cell survival *in vitro* and *in vivo*. Targeting UCKL-1 and decreasing its expression in tumor cells may be an effective method to decrease tumor survival and inhibit metastasis. Our study characterizing UCKL-1 as a uridine-cytidine kinase opens the door for the targeted manipulation of UCKL-1 as a cancer therapeutic and additional target for pyrimidine salvage inhibition.

Materials and methods

Cell cultures and protein extraction

The human glioblastoma U-87 cell line, human erythroleukemia K562 cell line, human T cell leukemia Jurkat cell line, and mouse lymphoma YAC-1 cell line were all purchased from American Type Culture Collection (ATCC). Additional cell lines were graciously provided by the following individuals: the two human breast cancer cell lines, MDA-MB-231 and MCF-7, were provided by Dr. Ratna Ray of Saint Louis University (Saint Louis, MO); the human liver carcinoma cell line, Huh-7, was provided by Dr. John Tavis of Saint Louis University; and the human bone osteosarcoma cell line, U-2 OS, was provided by Dr. Susana Gonzalo-Hervas of Saint Louis University.

K562, Jurkat, and YAC-1 were cultured in RPMI-1640 media supplemented with 7.5% heat-inactivated fetal bovine serum (FBS), 1% L-glutamine and 1% penicillin-streptomycin. All other cell lines were cultured in

DMEM high glucose supplemented with 10% FBS, 1% L-glutamine, and 1% penicillin-streptomycin. All cells were maintained in an atmosphere of 5% CO₂ at 37°C with 5% relative humidity. Cell counts were determined using a hemocytometer. Cell viability was determined using trypan blue dye exclusion (MilliporeSigma, Burlington, MA). Whole cell lysates were prepared using RIPA buffer (MilliporeSigma) with protease inhibitors and centrifuged at 12 000g for 10 min. Protein concentration was determined using Pierce™ bicinchoninic acid (BCA) Protein Assay (Thermo Fisher Scientific).

K562 cells expressing GFP were generated for *in vivo* studies. The cells were transfected with a pcDNA3 vector (Invitrogen, Carlsbad, CA) containing the GFP gene cloned from the pEGFP-N1 vector (Clontech, Mountain View, CA) as previously described [15]. GFP expression was verified by fluorescence microscopy, flow cytometry, and polymerase chain reaction (PCR).

Cloning and expression of human UCKL-1 and UCK2 in bacteria

The UCKL-1 construct was designed using cDNA from the pFlag-UCKL1 plasmid previously created by our lab [10]. The UCK2 construct was designed from cDNA generously provided by Dr. A.B.P. Van Kuilenburg of the Academisch Medisch Centrum (Amsterdam, The Netherlands). The targeted genes were amplified using PCR. Oligonucleotide primers flanking UCKL-1 and UCK2 (Table 2) were designed with *Bam*HI and *Xho*I restriction enzyme sites synthesized by Integrated DNA Technologies (Coralville, IA). The cDNAs were expressed with both an N-terminal and C-terminal polyhistidine (His) tag and cloned into the restriction enzyme sites of *Bam*HI and *Xho*I in pET32b plasmid vector.

The plasmids were transformed into *Escherichia coli* XL-10 Ultracompetent cells (Agilent Technologies, Santa Clara, CA). Plasmids from multiple colonies were sent for sequencing (Retrogen, San Diego, CA). The correct plasmids were then transformed into *E. coli* BL21-DE3 competent cells (New England Biolabs, Ipswich, MA), and colonies inoculated in 10 ml LB media supplemented with 100 µg/ml ampicillin. Bacteria were diluted in 50% glycerol and stored at -80°C.

Protein purification

Liquid bacterial cultures (10 ml) with 100 µg/ml ampicillin were inoculated using glycerol stocks of bacteria expressing either UCKL-1 or UCK2 and incubated at 37°C with shaking, overnight. The following day, overnight cultures were diluted 10-fold and maintained at 37°C until an optical density (OD₆₀₀) of 0.5–0.6 was reached. The cultures were then induced with isopropyl-β-D-1-thiogalactopyranoside (IPTG) at 20°C overnight (UCKL-1 = 100 µM IPTG; UCK2 = 50 µM IPTG). Cell pellets were harvested and stored at -80°C for later purification.

Bacteria expressing UCK2 were lysed using B-PER™, Complete Bacterial Protein Extraction Reagent, (Thermo Fisher Scientific) 5 ml per gram of biomass. The pellet was vortexed and incubated at room temperature for 15 min. Protein was extracted via sonication; the soluble fraction was obtained after high-speed centrifugation of the lysate. Bacteria expressing UCKL-1 were lysed using 5 ml urea lysis buffer per gram of biomass. The urea lysis buffer contained 4 M urea, 2 M thiourea, 4% CHAPS, 1% DTT, and 50 mM Tris, pH 8.0. The cell pellet was vortexed and incubated at room temperature for 15 min. Protein was extracted by sonication; the soluble fraction was collected after high-speed centrifugation of the lysate.

Purification of His-tagged UCKL-1 and UCK2 was accomplished using the ÄKTA pure chromatography system (Cytiva Life Sciences, Marlborough, MA). The cleared lysate was loaded onto a nickel affinity column and washed with 0.5 M sodium chloride (NaCl), 5 mM imidazole, and 20 mM monosodium phosphate (NaH₂PO₄), pH 7.4. After washing, the bound protein was eluted with a linear gradient of 100 mM–500 mM imidazole. The fractions containing the targeted protein were pooled, concentrated, and buffer exchanged to

Table 2 PCR primers

Primers	Sequences 5'→3', restriction enzyme site (underlined)
UCKL-1 (+)	AGTCAGGGATCCAATGGCTGCGCCCCCGGC, <i>Bam</i> HI
UCKL-1 (-)	AGTCAGCTCGAGACCCGTGTAGGCCAXTTCCCTCC, <i>Xho</i> I
UCK2 (+)	AGTCAGGGATCCAATGGCCGGGGACAGCGAG, <i>Bam</i> HI
UCK2 (-)	AGTCAGCTCGAGATGCGGCCTGCTGCTGG, <i>Xho</i> I

150 mM NaCl and 20 mM NaH₂PO₄, pH 7.4 using Amicon® Ultra-15 10K centrifugal filter device (Millipore Sigma). The purity of the fractions was assessed by sodium dodecyl sulfate polyacrylamide gel electrophoresis. Protein concentrations were determined with Pierce™ BCA Protein Assay. The purified proteins were diluted 1:1 in buffer containing: 40% glycerol (v/v), 200 mM NaCl, 200 μM phenylmethylsulfonyl fluoride (PMSF), and 20 mM NaH₂PO₄, pH 7.4, aliquoted and stored at –80°C.

Immunoblotting

Purified UCKL-1 and UCK2 proteins (100 ng) and whole cell lysates from various tumor cell lines (30 μg) were run on 10% SDS-polyacrylamide gels, then transferred to polyvinylidene difluoride (PVDF) membranes. Membranes were blocked with 5% milk blocking buffer for 30 min, then incubated with primary antibodies overnight at 4°C. After overnight incubation, membranes were washed three times for 10 min each in 0.1% Tris-buffered saline with Tween 20 (TBST) followed by 1 h incubation with horseradish peroxidase (HRP)-conjugated secondary antibodies at room temperature. Membranes were washed an additional three times for 10 min each in TBST and then protein bands detected using Clarity™ Western ECL substrate (Bio-Rad, Hercules, CA). Blots were imaged on ChemiDoc imaging system (Bio-Rad). Additionally, a 10% SDS-polyacrylamide gel with 100 ng of purified UCKL-1 and UCK2 was treated with Coomassie blue stain for 10 min and then rinsed with Destain solution overnight.

The following antibodies were used for immunoblotting: UCKL-1 (B-11) mouse monoclonal (1: 1000 dilution, Santa Cruz); UCKL1 [EPR7384] rabbit monoclonal (1: 1000 dilution, Abcam); UCK2 rabbit polyclonal (1: 1000 dilution, Thermo Fisher Scientific); UCK1 rabbit polyclonal (1: 1000 dilution, Thermo Fisher Scientific); 6x-His tag mouse monoclonal (HIS.H8), HRP (1: 10 000 dilution, Thermo Fisher Scientific); and β-actin mouse monoclonal (1: 5000 dilution, Millipore Sigma). The following secondary antibodies were used for western blotting: HRP-conjugated goat anti-mouse IgG (1: 10 000 dilution) and HRP-conjugated goat anti-rabbit IgG (1: 10 000 dilution, Cell Signaling Technology).

Enzymatic assays

UCKL-1 and UCK2 kinase activity was measured using the ADP-Glo™ Kinase Assay system from Promega (Madison, WI). UCK2 assays were performed in 10 μl containing 50 mM Tris, pH 7.5, 5 mM MgCl₂, 2 mM DTT, and 0.5 mg/ml bovine serum albumin (BSA). The final concentration of UCK2 was 1 ng, ATP concentration was 100 μM, and substrate concentration began at 50 μM. Assays were initiated by addition of substrate to enzyme, and reactions allowed to proceed for up to 3 h at room temperature.

UCKL-1 assays were performed in 10 μl containing 50 mM Tris, pH 6.0, 5 mM MgCl₂, 2 mM DTT, 0.5 mg/ml BSA, 12 mM NaCl, and 100 nM CaCl₂. UCKL-1 final concentration was 500 ng, ATP concentration was 100 μM, and substrate concentration began at 8 μM. Assays were initiated by addition of substrate to enzyme, and reactions incubated for up to 3 h at 37°C.

All reactions were terminated by addition of ADP-Glo Reagent (10 μl) and incubated at room temperature for 40 min. Then 20 μl Kinase Detection Reagent was added to elicit luminescence. After 45 min incubation at room temperature, luminescence was measured on a BioTek Synergy 2 microplate reader (BioTek, Winooski, VT). ADP formation was calculated using an ATP-to-ADP conversion curve. All assays were replicated a minimum of three times.

Nucleofection (transfection) with siRNA

Nucleofection was performed with a Lonza Nucleofection I device and an optimized kit, Cell Line Nucleofector Kit V (Lonza, Germany), using programs T-16 (K562) and X-5 (YAC-1). The UCKL-1 siRNA duplexes were obtained from Invitrogen and resuspended per manufacturer's protocol. The UCKL-1 siRNA generated for *in vitro* experiments was targeted to region 1553 of mouse UCKL-1. YAC-1 cells were nucleofected with 2 μM of either siUCKL-1 or siGFP control. Down-regulation of UCKL-1 gene expression was confirmed by quantitative PCR at various times post-nucleofection.

In vivo siRNA from Invitrogen targeted region 1305 of UCKL-1, which is conserved in all UCKL-1 splice variants. The ability of the *in vivo* siRNA to diminish UCKL-1 expression was tested *in vitro* before use [15]. Scrambled siRNA was prepared as a negative control. The *in vivo* siRNA was provided in the 2'-deprotected form, and along with other processing, is formulated for increased stability *in vivo*.

Cell and tissue RNA was isolated using Qiagen RNeasy Kit (Qiagen, Valencia CA) and cDNA prepared using the Superscript II Kit (Invitrogen). Expression of UCKL-1 was determined by qPCR using UCKL-1

primers (forward primer GTCGCGACGAGTTCATCTC and reverse primer GTCCTCAGGCACGTCGTGGT) that are homologous to both mouse and human UCKL-1. Expression levels were normalized to 18s rRNA. The Taqman Gene Expression Master Mix (Applied Biosystems, Foster City, CA) along with Applied Biosystems 7500 system was utilized for real-time PCR analysis.

Caspase assay

Caspase activity was assessed using the Caspase-Glo 3/7 Luminescence Assay Kit (Promega). One day after nucleofection with either siUCKL-1 or siGFP control, YAC-1 cells (0.15×10^5) were spun down and resuspended in 75 μ l RPMI media containing 3.75% serum. The cells were then aliquoted into three wells of a white walled 96-well plate. Caspase-Glo (25 μ l) was added to all wells and mixed. Samples were incubated for 30 min at room temperature and analyzed for luminescence using a Victor 1420 Multilabel Counter (Wallac/PerkinElmer, Waltham, MA). Samples were analyzed in triplicate, along with a media control. Luminescence values obtained were averaged and the media control subtracted. The percent fold increase in caspase activity over time was calculated relative to the control group.

Treatment of tumor-bearing NOD-scid IL2R γ ^{null} (NSG) mice with siRNA

Immunodeficient NSG mice were acquired from Dr. Guangyong Peng of Saint Louis University and were originally obtained from Jackson Laboratories (stock number: 005557, NOD.Cg-Prkdc^{scid}IL2rg^{tmWjl}/SzJ). All animal experiments were carried out in the animal care facilities at Saint Louis University School of Medicine. Mice were injected subcutaneously in the rear flank, either unilaterally or bilaterally, with 10^6 K562-GFP cells suspended in 50 μ l PBS + 50 μ l Matrigel. The unilateral model was used for the metastasis and dissemination study, whereas the bilateral model was used for the primary tumor growth study. Tattoo ink was used to identify the site of injection to aid in proper injection of the siRNA.

Once tumors were established (day 8), mice were briefly anesthetized with isoflurane (1–3%) via a precision vaporizer with waste gas scavenging system prior to injection with siRNA. Mice were injected with either 8 μ g sicontrol or siUCKL-1 in 50 μ l PBS at two separate sites within the tumor. For mice with bilateral tumors, one tumor was injected with control siRNA, while the other tumor was injected with UCKL-1 siRNA. Tumors were measured and injected every other day for one week. Fifteen days post-tumor inoculation, mice were sacrificed by asphyxiation via CO₂ inhalation using a gas compressed source with a displacement rate of 30–70% of the chamber volume per minute until breathing stopped, followed by cervical dislocation. Blood was obtained from the heart immediately after sacrifice. Fluorescence within each mouse was measured via the IVIS Spectrum *in vivo* imaging system. Fluorescence intensity of isolated tumors was also evaluated using IVIS. The level of GFP expression was calculated above background fluorescence. After visualization, tumors and additional organs were collected to measure levels of GFP by qPCR.

Lung metastasis and tumor dissemination in the blood was evaluated by RT-qPCR using GFP-specific Taqman primer/probes. Samples were run on a 7500 Applied Biosystems real-time PCR system. Change in C_t was calculated using 18s as a housekeeping control.

Terminal deoxynucleotidyl transferase dUTP nick end labeling (TUNEL) staining of tumor sections

Primary tumors were isolated from NSG mice on day of sacrifice (day 15). Tumors were weighed, measured, and placed in 10% formalin. Tumors were dehydrated overnight and paraffin embedded. The tumors were sectioned and placed on glass slides. Slide sections were dewaxed and rehydrated with xylene and ethanol in decreasing percentages. The tumor sections then underwent antigen retrieval. 1X Diva DeCloaker (Biocare Medical, Concord, CA) was added to the sections and rapidly heated in a pressure cooker. Slides were then cooled and washed twice in dH₂O. Roche In Situ Cell Death Detection Kit (Indianapolis, IN) was used for TUNEL staining to measure apoptosis. Samples treated with DNase served as positive controls, while negative controls contained the label solution only. Six fields were fluorescently imaged for each sample on an Olympus BX41 microscope with a DP72 Olympus digital camera. All samples were normalized to each negative control threshold and analyzed using Metamorph software (Molecular Devices, Sunnyvale, CA) and Image J (NIH). Hematoxylin and Eosin staining was performed on an additional section of primary tumors.

Statistical analysis

All data were analyzed using GraphPad Prism software (San Diego, CA) or Microsoft Excel (Redmond, WA). A Student's *t*-test and a one-way analysis of variance (ANOVA) were used for statistical analysis with a *P* value ≤ 0.05 considered statistically significant.

Data Availability

All primary data and constructs are freely available upon request to the corresponding author.

Competing Interests

The authors declare that there are no competing interests associated with the manuscript.

Funding

This material is based upon work supported by the Department of Veterans Affairs, Biomedical Laboratory Research and Development Service (VA Merit Grant I01 BX000705) and Saint Louis University.

CRedit Author Contribution

Jacki Kornbluth: Conceptualization, Resources, Data curation, Supervision, Funding acquisition, Validation, Methodology, Writing — review and editing. **Emily Matchett:** Investigation, Methodology, Writing — original draft. **Elise C. Ambrose:** Formal analysis, Investigation, Writing — original draft.

Ethics Approval

This study was carried out in strict accordance with the provisions of the USDA Animal Welfare Act Regulations and Standards, PHS policy, recommendations in the Guide for the Care and Use of Laboratory Animals, and VA policy. All *in vivo* studies performed in mice were approved by both the Saint Louis University and the VA St. Louis Health Care System Institutional Animal Care and Use Committees (SLU IACUC Protocol #1287; VA ACORP Protocol #1166443).

Acknowledgements

The authors would like to thank Paul Willard and Donald Lawrence for their technical support and input, the Research Microscopy Core, and the Comparative Medicine staff at Saint Louis University for their expertise and support.

Abbreviations

GFP, green fluorescent protein; His, polyhistidine; IMAC, immobilized metal affinity chromatography; IPTG, isopropyl- β -D-1-thiogalactopyranoside; NK, natural killer; NKLAM, natural killer lytic-associated molecule; NSG, NOD-scid-IL2R γ^{null} ; siRNA, small interfering RNA; TUNEL, terminal deoxynucleotidyl transferase dUTP nick end labeling; UCK, uridine/cytidine kinase; UCKL, uridine/cytidine kinase-like; UPRT, uracil phosphoribosyltransferase.

References

- 1 Qian, Y., Ding, Q., Li, Y., Zou, Z., Yan, B. and Ou, L. (2014) Phosphorylation of uridine and cytidine by uridine-cytidine kinase. *J. Biotechnol.* **188**, 81–87 <https://doi.org/10.1016/j.jbiotec.2014.08.018>
- 2 Cheng, N., Payne, R.C. and Traut, T.W. (1986) Regulation of uridine kinase: evidence for a regulatory site. *J. Biol. Chem.* **261**, 13006–13012 [https://doi.org/10.1016/S0021-9258\(18\)69262-2](https://doi.org/10.1016/S0021-9258(18)69262-2)
- 3 Van Rompay, A.R., Norda, A., Lindén, K., Johansson, M. and Karlsson, A. (2001) Phosphorylation of uridine and cytidine nucleoside analogs by two human uridine-cytidine kinases. *Mol. Pharmacol.* **59**, 1181–1186 <https://doi.org/10.1124/mol.59.5.1181>
- 4 Suzuki, N.N., Koizumi, K., Fukushima, M., Matsuda, A. and Inagaki, F. (2004) Structural basis for the specificity, catalysis, and regulation of human uridine-cytidine kinase. *Structure* **12**, 751–764 <https://doi.org/10.1016/j.str.2004.02.038>
- 5 Van Rompay, A.R., Johansson, M. and Karlsson, A. (1999) Phosphorylation of deoxycytidine analog monophosphates by UMP-CMP kinase: molecular characterization of the human enzyme. *Mol. Pharmacol.* **56**, 562–569 <https://doi.org/10.1124/mol.56.3.562>
- 6 Van Kuilenburg, A.B.P. and Meinsma, R. (2016) The pivotal role of uridine-cytidine kinases in pyrimidine metabolism and activation of cytotoxic nucleoside analogues in neuroblastoma. *Biochim. Biophys. Acta* **1862**, 1504–1512 <https://doi.org/10.1016/j.bbadis.2016.05.012>
- 7 Murata, D., Endo, Y., Obata, T., Sakamoto, K., Syouji, Y., Kadohira, M. et al. (2004) A crucial role of uridine/cytidine kinase 2 in antitumor activity of 3' ethynyl nucleosides. *Drug Metab. Disp.* **32**, 1178–1182 <https://doi.org/10.1124/dmd.104.000737>
- 8 Meinsma, R. and Van Kuilenburg, A.B.P. (2016) Purification, activity, and expression levels of two uridine-cytidine kinase isoforms in neuroblastoma cell lines. *Nucleosides Nucleotides Nucleic Acids* **35**, 613–618 <https://doi.org/10.1080/15257770.2015.1124998>

- 9 Kashuba, E., Kashuba, V., Sandalova, T., Klein, G. and Szekely, L. (2002) Epstein-barr virus encoded nuclear protein EBNA-3 binds a novel human uridine kinase/uracil phosphoribosyltransferase. *BMC Cell Biol.* **3**, 23 <https://doi.org/10.1186/1471-2121-3-23>
- 10 Fortier, J.M. and Kornbluth, J. (2006) NK lytic-associated molecule, involved in NK cytotoxic function, is an E3 ligase. *J. Immunol.* **176**, 6454–6463 <https://doi.org/10.4049/jimmunol.176.11.6454>
- 11 Hoover, R.G., Gullickson, G. and Kornbluth, J. (2012) Natural killer lytic-associated molecule plays a role in controlling tumor dissemination and metastasis. *Front. Immunol.* **3**, 393 <https://doi.org/10.3389/fimmu.2012.00393>
- 12 Mukhopadhyay, D. and Riezma, H. (2007) Proteasome-independent functions of ubiquitin in endocytosis and signaling. *Science* **315**, 201–205 <https://doi.org/10.1126/science.1127085>
- 13 Lawrence, D.W., Willard, P.A., Cochran, A.M., Matchett, E.C. and Kornbluth, J. (2020) Natural killer lytic-associated molecule (NKLAM): an E3 ubiquitin ligase with an integral role in innate immunity. *Front. Physiol.* **11**, 573372 <https://doi.org/10.3389/fphys.2020.573372>
- 14 Glickman, M.H. and Ciechanover, A. (2002) The ubiquitin-proteasome proteolytic pathway: destruction for the sake of construction. *Physiol. Rev.* **82**, 373–428 <https://doi.org/10.1152/physrev.00027.2001>
- 15 Ambrose, E.C. and Kornbluth, J. (2009) Downregulation of uridine-cytidine kinase like-1 decreases proliferation and enhances tumor susceptibility to lysis by apoptotic agents and natural killer cells. *Apoptosis* **14**, 1227–1236 <https://doi.org/10.1007/s10495-009-0385-z>
- 16 Gullickson, G., Ambrose, E.C., Hoover, R.G. and Kornbluth, J. (2016) Uridine cytidine kinase like-1 enhances tumor cell proliferation and mediates protection from natural killer-mediated killing. *Int. J. Immunol. Immunother.* **3**, 018 <https://doi.org/10.23937/2378-3672/1410018>
- 17 Cheng, W.S., Tao, H., Hu, E.P., Liu, S., Cai, H.R., Tao, X.L. et al. (2014) Both genes and lncRNAs can be used as biomarkers of prostate cancer by using high throughput sequencing data. *Eur. Rev. Med. Pharm. Sci.* **18**, 3504–3510 PMID: 25491628
- 18 Geiger, T., Madden, S.F., Gallagher, W.M., Cox, J. and Mann, M. (2012) Proteomic portrait of human breast cancer progression identifies novel prognostic markers. *Cancer Res.* **72**, 2428–2439 <https://doi.org/10.1158/0008-5472.CAN-11-3711>
- 19 Long, N.P., Lee, W.J., Huy, N.T., Lee, S.J., Park, J.H. and Kwon, S.W. (2016) Novel biomarker candidates for colorectal cancer metastasis: a meta-analysis of *in vitro* studies. *Cancer Informatics* **15**, 11–17 <https://doi.org/10.4137/CIN.S40301>
- 20 Buivydiene, A., Liakina, V., Valantinas, J., Norkuniene, J., Mockiene, E., Jokubauskiene, S. et al. (2017) Expression levels of the uridine-cytidine kinase like-1 protein as a novel prognostic factor for hepatitis C virus-associated hepatocellular carcinomas. *Acta Naturae* **9**, 34 <https://doi.org/10.32607/20758251-2017-9-3-108-114>
- 21 Wang, H., Wang, X., Xu, L., Zhang, J. and Cao, H. (2020) High expression levels of pyrimidine metabolic rate-limiting enzymes are adverse prognostic factors in lung adenocarcinoma: a study based on The Cancer Genome Atlas and Gene Expression Omnibus datasets. *Purinergic Signal.* **16**, 347–366 <https://doi.org/10.1007/s11302-020-09711-4>
- 22 Shen, G., He, P., Mao, Y., Li, P., Luh, F., Ding, G. et al. (2017) Overexpression of uridine-cytidine kinase 2 correlates with breast cancer progression and poor prognosis. *J. Breast Cancer* **20**, 132–141 <https://doi.org/10.4048/jbc.2017.20.2.132>
- 23 Zhou, Q., Jiang, H., Zhang, J., Yu, W., Zhou, Z., Huang, P. et al. (2018) Uridine-cytidine kinase 2 promotes metastasis of hepatocellular carcinoma cells via the Stat3 pathway. *Cancer Manag. Res.* **10**, 6339–6355 <https://doi.org/10.2147/cmar.s182859>
- 24 Zegzouti, H., Zdanovskaia, M., Hsiao, K. and Goueli, S.A. (2009) ADP-Glo: a bioluminescent and homogeneous ADP monitoring assay for kinases. *Assay Drug Dev. Tech.* **7**, 560–572 <https://doi.org/10.1089/adt.2009.0222>
- 25 Okesli-Armlovich, A., Gupta, A., Jimenez, M., Auld, D., Liu, Q., Bassik, M.C. et al. (2019) Discovery of small molecule inhibitors of human uridine-cytidine kinase 2 by high-throughput screening. *Bioorg. Med. Chem. Lett.* **29**, 2559–2564 <https://doi.org/10.1016/j.bmcl.2019.08.010>
- 26 Villela, A.D., Ducati, R.G., Rosado, L.A., Bloch, C.J., Prates, M.V., Gonçalves, D.C. et al. (2013) Biochemical characterization of uracil phosphoribosyltransferase from *Mycobacterium tuberculosis*. *PLoS ONE* **8**, e56445 <https://doi.org/10.1371/journal.pone.0056445>
- 27 Carter, D., Donald, R.G.K., Roos, D. and Ullman, B. (1997) Expression, purification, and characterization of uracil phosphoribosyltransferase from *Toxoplasma gondii*. *Mol. Biochem. Parasitol.* **87**, 137–144 [https://doi.org/10.1016/S0166-6851\(97\)00058-3](https://doi.org/10.1016/S0166-6851(97)00058-3)
- 28 Rafiqul Islam, M., Kim, H., Kang, S.W., Kim, J.S., Jeong, Y.M., Hwang, H.J. et al. (2007) Functional characterization of a gene encoding a dual domain for uridine kinase and uracil phosphoribosyltransferase in *Arabidopsis thaliana*. *Plant Mol. Biol.* **63**, 465–477 <https://doi.org/10.1007/s11103-006-9101-3>
- 29 Li, J., Huang, S., Chen, J., Yang, Z., Fei, X., Zheng, M. et al. (2007) Identification and characterization of human uracil phosphoribosyltransferase (UPRTase). *J. Hum. Genet.* **52**, 415–422 <https://doi.org/10.1007/s10038-007-0129-2>
- 30 Wang, W., Cui, J., Ma, H., Lu, W. and Huang, J. (2021) Targeting pyrimidine metabolism in the era of precision cancer medicine. *Front. Oncol.* **11**, 684961 <https://doi.org/10.3389/fonc.2021.684961>
- 31 Walter, M. and Herr, P. (2022) Rediscovery of pyrimidine salvage as target in cancer therapy. *Cells* **11**, 739 <https://doi.org/10.3390/cells11040739>
- 32 Yamaguchi, N., Weinberg, E.M., Nguyen, A., Liberti, M.V., Goodarzi, H., Janjigian, Y.Y. et al. (2019) PCK1 and DHODH drive colorectal cancer liver metastatic colonization and hypoxic growth by promoting nucleotide synthesis. *Elife* **8**, e52135 <https://doi.org/10.7554/eLife.52135>
- 33 Xiang, J., Chen, C., Liu, R., Gou, D., Chang, L., Deng, H. et al. (2021) Gluconeogenic enzyme PCK1 deficiency promotes CHK2 O-GlcNAcylation and hepatocellular carcinoma growth upon glucose deprivation. *J. Clin. Invest.* **131**, e144703 <https://doi.org/10.1172/JCI144703>
- 34 Zhou, Y., Tao, L., Zhou, X., Zuo, Z., Gong, J., Liu, X. et al. (2021) DHODH and cancer: promising prospects to be explored. *Cancer Metab.* **9**, 22 <https://doi.org/10.1186/s40170-021-00250-z>
- 35 Sykes, D.B., Kfoury, Y.S., Mercier, F.E., Wawer, M.J., Law, J.M., Haynes, M.K. et al. (2016) Inhibition of dihydroorotate dehydrogenase overcomes differentiation blockade in acute myeloid leukemia. *Cell* **167**, 171–186 <https://doi.org/10.1016/j.cell.2016.08.057>
- 36 Sarkisjan, D., Julsin, J.R., Smid, K., De Klerk, D., Van Kuilenberg, A.B.P., Meinsma, R. et al. (2016) The cytidine analog fluorocyclopentenylcytosine (RX-3117) is activated by uridine-cytidine kinase 2. *PLoS ONE* **11**, e0162901 <https://doi.org/10.1371/journal.pone.0162901>
- 37 Balboni, B., Hassouni, B.E., Honeywell, R.J., Sarkisjan, D., Giovannetti, E., Poore, J. et al. (2019) RX-3117 (fluorocyclopentenyl cytosine): a novel specific antimetabolite for selective cancer treatment. *Expert Opin. Investig. Drugs* **28**, 311–322 <https://doi.org/10.1080/13543784.2019.1583742>
- 38 Liu, Q., Gupta, A., Okesli-Armlovich, A., Qiao, W., Fischer, C.R., Smith, M. et al. (2020) Enhancing the antiviral efficacy of RNA-dependent RNA polymerase inhibition by combination with modulators of pyrimidine metabolism. *Cell Chem. Biol.* **27**, 668–677 <https://doi.org/10.1016/j.chembiol.2020.05.002>